Chemical imaging of insulators by STM

J. Viernow,* D. Y. Petrovykh, A. Kirakosian, J.-L. Lin, F. K. Men,† M. Henzler,* and F. J. Himpsel
Department of Physics, University of Wisconsin Madison, 1150 University Avenue, Madison, Wisconsin 53706-1390
(Received 1 December 1998)

Nanostructures of CaF_2 and CaF_1 on Si(111) are used to demonstrate a chemical imaging method for insulators. Chemical sensitivity is achieved in scanning tunneling microscopy via a sharp drop of the tunneling current for bias voltages below the conduction-band minimum. This imaging method has a spatial resolution of better than 1 nm and distinguishes different oxidation states. A resonance is found in $(dI/dV)/(I/V)$ at the conduction-band minimum that enables an accurate determination of its position. We observe enhancements by up to a factor of 5 and absolute values in the range of 20–50, compared to 1 for an Ohmic metal. A minimal model is given, explaining the resonance in terms of tunneling across a thin insulator film. These methods should be generally applicable for determining local Schottky barriers and band offsets in nanostructures and for chemically selective imaging of insulators and wide-gap semiconductors. [S0163-1829(99)07215-X]

I. CHEMICAL IMAGING IN SCANNING TUNNELING MICROSCOPY (STM)

Chemical imaging has been a long-standing goal in high-resolution microscopy.[1–5] The finer the resolution becomes, the more difficult it is to obtain chemical information. Approaching the atomic resolution limit, there are only a few atoms within the resolution volume that can be sampled. In transmission electron microscopy, the energy loss spectrum has become a tool for identifying different chemical species.[2] In STM such a general method has not been found yet, although a variety of effects can lead to chemical contrast in specific cases.[1] For metals, two techniques have been employed[3,4] utilizing the work function as identifier. One is based on resonant tunneling into image states,[3] the other on a measurement of the tunneling barrier.[4] On semiconductor surfaces, specific broken bond orbitals are distinguishable in the gap[5] but their identity needs to be analyzed in detail before a chemical assignment can be made. Differences in the electron/hole confinement can provide contrast in cross-sectional STM.[6,7] A general method that works for insulators has been lacking so far. It is desirable to have a complete set of tools identifying all classes of materials, particularly in the rapidly growing field of self-assembled nanostructures. In future nanodevices, insulators will necessarily play a crucial role in electrically separating wires or dots. In addition, the band structure of semiconductors and insulators is modified in nanometer-size objects,[8] making a local, *in situ* band measurement quite valuable. Local variations in the position of the conduction-band minimum (CBM) are also significant in wide-gap semiconductors, which have attracted interest as emitters of blue light.

We have achieved chemical selectivity between different insulators and even different oxidation states of the same element. Essentially, we take advantage of a large jump in the conductivity at the CBM of insulators. The chemical identifier is the energy of the CBM relative to the Fermi level E_F. It represents the analog to the work function that has been used to identify metals.[3,4] We are able to discriminate between Si, CaF_2, and CaF_1 in nanowire and island structures grown epitaxially on stepped Si(111). Height differences between terraces and across individual terraces are eliminated. The local conduction-band minima are determined with a spatial resolution of 1 nm making the spectroscopic sampling of individual nanostructures a reality.

II. CaF_2/Si(111) SYSTEM

CaF_2 on Si(111) has been selected as a prototype of a well-defined, epitaxial insulator structure. Previous work[9–13] has established two types of atomically sharp interfaces, one F terminated, the other Ca terminated. The F-terminated interface contains a full F-Ca-F triple layer that is characteristic of the CaF_2(111) structure. The F-layer adjacent to Si desorbs at ≈700 °C and a Si-Ca-F interface is formed, where the second valence of Ca is taken up by the broken surface bond of Si(111). This CaF_1 layer has an optical band gap[11] of only 2.4 eV, as opposed to the 12-eV gap of CaF_2. When going from a flat Si(111) surface to a nanostructured topography at vicinal Si(111) surfaces,[14] complex growth modes start to appear, such as islands attached to step edges, bunched steps, stripes, and double-layer structures. Determining the local chemistry in this case requires an analysis tool that operates on the nanometer scale and ignores these topographical variations.

The calcium fluoride samples in this study comprise the Ca-terminated interface as well as the F-terminated interface. The first type of the interface was obtained on a Si(111) surface miscut by 1.1° towards the $[\overline{1}\,1\,2]$ azimuth, with 1.5 triple layers of CaF_2 deposited at 610 °C and postannealed at 830 °C for $\frac{1}{2}$ min and at 700 °C for 4 min. The sample with the F-terminated interface was grown on a Si(111) surface miscut by 1.3° towards the opposite azimuth, i.e., $[11\overline{2}]$, with $\frac{1}{3}$ of a triple layer of CaF_2 deposited at 650 °C.

III. CHEMICAL IMAGING BY SPECTROSCOPIC STM

Before getting into the details of chemically selective tunneling, it is useful to recall how tunneling into insulators becomes possible. As shown previously,[15–20] electrons are able to tunnel from the tip into the conduction-band minimum of an insulator when applying a sufficiently large, posi-

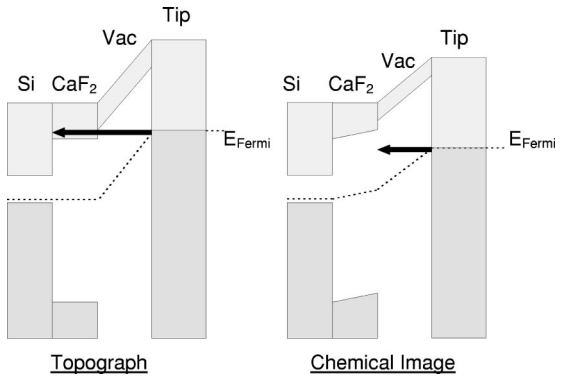

FIG. 1. Schematic of chemically-selective tunneling into insulator films, using CaF_2 on Si(111) as an example: left, stabilizing the tip at a sample bias that allows tunneling of electrons from the tip into the CBM of the insulator; right, acquiring a current image at a bias where electrons from the tip enter the gap of the insulator. The insulator appears dark.

tive sample bias (Fig. 1, left). Electrons injected into the conduction-band pass through the insulator and prevent it from charging, as long as the film is thinner than the mean free path at the CBM (typically in the 10-nm range). In the specific cases considered here, the CBM lies about 3–5 eV above E_F for CaF_2 and 1.4–1.8 eV above E_F for CaF_1.[21] In CaF_2, a stable tunneling current is obtained at a sample bias voltage of $\geqslant 4$ V (typically 0.3–1.0 nA). Attempts to stabilize the tunneling current at a bias voltage below the CBM causes the tip to approach the underlying Si and to pick up insulating CaF_2 debris. The voltage drop across the CaF_2 layer is drawn differently for the two cases in Fig. 1. It is small when tunneling above the conduction-band minimum (Fig. 1, left), where CaF_2 is conducting. For tunneling into the gap (Fig. 1, right), we are almost in the electrostatic limit. Part of the applied voltage drops in the insulator. It is determined by the electric field of the tip, reduced by the dielectric constant $\epsilon = 7$ of CaF_2.

For chemical imaging the feedback loop is turned off and current-voltage curves are acquired at each image point. Figure 2 shows such $I(V)$ data, averaged over atomically-flat areas $3 \times 3\ \mathrm{nm}^2$ in size. Typically, $I(V)$ curves are taken at 400 image points in order to check for spatial homogeneity. In addition, the tip height is varied by changing the sample bias (different types of lines in Fig. 2). For each spectrum, the tip is stabilized near its highest voltage point, thereby avoiding overflow and underflow of the current. An approximate density of states can be derived[22–24] by calculating the differential conductance (dI/dV), or its normalized version $(dI/dV)/(I/V)$. The derivative is obtained from a cubic spline interpolation of the $I(V)$ data points. The conduction-band edges correspond to onsets in the (dI/dV) curves that become well-defined peaks in the normalized spectra. The onset behavior is reminiscent of data from semiconductors,[6,7,24] the peaks have not been observed before. This feature will be discussed in more detail in Sec. IV. From macroscopic techniques,[21] such as photoemission,[9–11] inverse photoemission,[12] and second-harmonic generation[11] one would expect a CBM at 3.6–3.8 eV above E_F for CaF_2. This is consistent with the peak at 3.7 eV for CaF_2 in Fig. 2. The peak at 2.3 eV for CaF_1 in Fig. 2 is higher than the

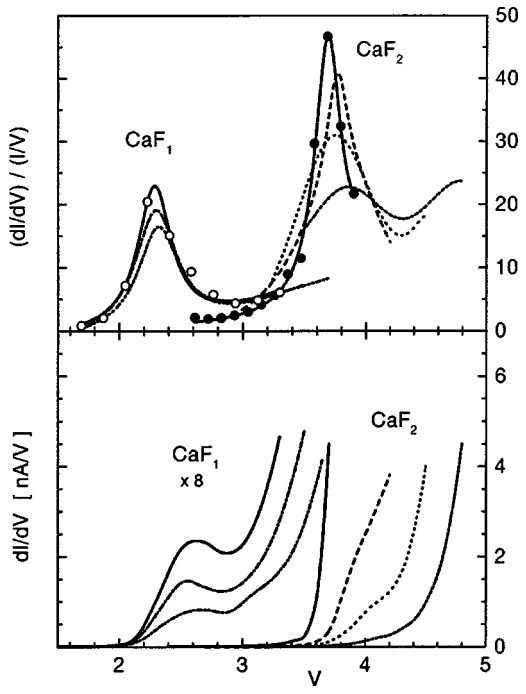

FIG. 2. Tunneling spectra of $CaF_1/Si(111)$ and $CaF_2/CaF_1/Si(111)$. Two sharp onsets in the (dI/dV) spectra characterize the respective conduction-band minima and provide chemical selectivity. The normalized $(dI/dV)/(I/V)$ spectra exhibit resonances at the CBM. Different line types represent different tip heights.

expected CBM of 1.4–1.8 eV for a CaF_1 layer but consistent with the CBM of the underlying Si along the [111] tunneling direction.[25]

For a chemical image it is not necessary to acquire a complete $I(V)$ curve at each pixel. A single voltage point per chemical species is enough, as demonstrated in Figs. 3 and 4. In Fig. 4, CaF_2 is distinguished from Si, in Fig. 3 from CaF_1. In both cases, the tip is stabilized at a bias corresponding to the CBM of CaF_2. The chemical image is acquired at a 0.5–2 eV lower bias. A larger bias reduction provides better chemical contrast at the expense of a lower absolute current. In such chemical images the height difference between Si steps is eliminated. In fact, the chemical contrast is opposite to the topographic contrast in Fig. 3: CaF_2 stripes appear bright in the topographic image (top) but dark in the chemical images (bottom). The chemical composition of the surface determines the contrast exclusively, with CaF_2 being darkest, Si brightest, and CaF_1 in between.

The spatial resolution better than 1 nm, as demonstrated in Fig. 5 by a line scan across a chemical image of a small CaF_2 island on Si(111). It was grown at 550 °C, where the diffusion length is only a few nm. Taking the sharpness of the edges as criterion we find a spatial resolution of better than 1 nm. That makes it possible to determine the CBM of individual nanoclusters and other quantum structures. The energy shifts expected from confining electrons to nanometer-size objects are expected to be in the 0.1–1 eV range. For example, the difference between the lowest two states in a linear quantum well of length l and infinite depth is $(E_2 - E_1) = 3h^2/8ml^2$, which amounts to 1 eV for $l = 1$ nm. That should be easily resolvable with our technique

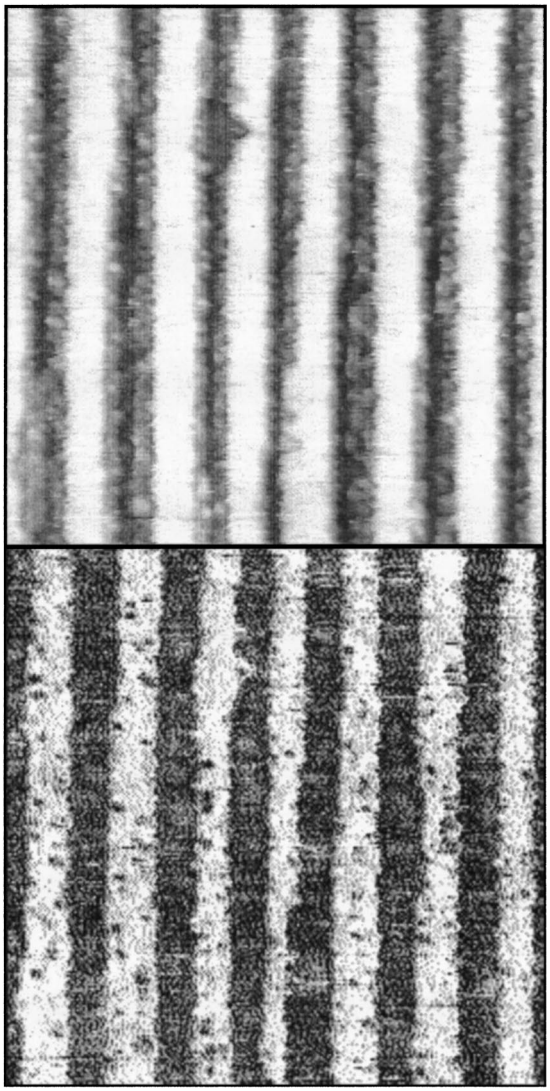

FIG. 3. Discrimination of CaF_1 from CaF_2 by chemically selective tunneling. Stripes of CaF_2 reside on top of a monolayer of CaF_1 that completely coats a stepped Si(111). Top: Topography obtained at a sample bias of +4.3 V with a tunneling current of 0.4 nA. Bottom: Chemical image, obtained from the tunneling current distribution at a sample bias of +3.8 V while stabilizing the tip height at +4.3 V. The patches with the higher band gap (CaF_2) appear dark, leading to an inversion of the topographic contrast. $100\times100\ nm^2$.

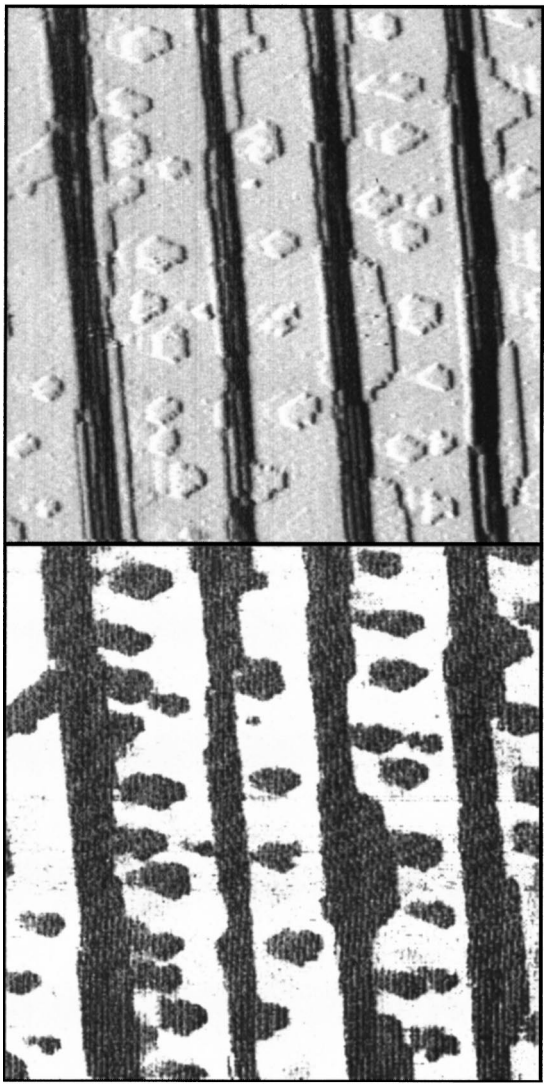

FIG. 4. Chemical distinction between CaF_2 and Si, using islands and stripes of CaF_2 on a Si(111) surface with bunched steps. Top: Topography obtained at a sample bias of +4 V with a tunneling current of 1 nA. The x derivative of the tip height is given, simulating side illumination from the left. Bottom: Chemical image, given by the tunneling current distribution at a sample bias of +2 V while stabilizing the tip height at a sample bias of +4 V. Electrons from the tip cannot enter the gap of CaF_2, resulting in a low current for CaF_2 patches (dark areas). $200\times200\ nm^2$.

thanks to the sharp resonances observed in Fig. 2.

IV. RESONANCE AT THE CONDUCTION-BAND MINIMUM

The $(dI/dV)/(I/V)$ tunneling spectra in Fig. 2 exhibit a surprising resonance at the conduction-band minimum (CBM). The peak is three times as high as the continuum above it for CaF_2 and five times as high for CaF_1. In search of an explanation for this phenomenon we consider several options.

a. Divergence of $(dI/dV)/(I/V)$ *at the band edge.* It has been pointed out that normalized scanning tunneling spectra of *bulk* semiconductors diverge at the conduction-band minimum.[24] The current I approaches zero faster than the differential conductance (dI/dV) when approaching the conduction-band edge from above. Inside the gap, $(dI/dV)/(I/V)$ is undetermined because $I=0$. We utilize *thin films*, where the tunneling current I remains finite inside the band gap. The states of the silicon substrate decay exponentially through the CaF_2 film, leaving a finite density of states at the CaF_2 surface available for tunneling. The normalization problems encountered with bulk semiconductors[24] are averted. We will develop a model for tunneling through a thin-film insulator film below that is based on established approaches for planar tunneling.[22–24] The outcome produces the observed resonances and even their absolute height, suggesting this as the most likely explanation.

b. Tip-surface interaction. Tip-induced modifications of

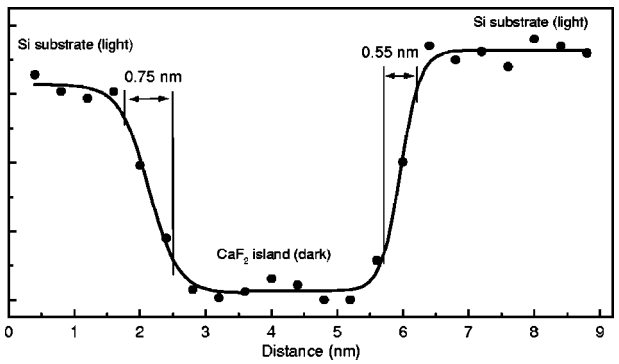

FIG. 5. Resolution test for chemical imaging of CaF_2 versus Si. A line scan across the chemical image of a CaF_2 island on Si gives a resolution of less than 1 nm (15–85% of the edge jump, corresponding to the full width at half-maximum of the derivative).

the band structure, such as tip-induced band bending, have been discussed in the context of semiconductors.[24] With ionic insulators, one might expect the electric field of the tip to influence the ions. In order to test for such effects, the spectra in Fig. 2 have been taken for different tip spacing by changing the sample bias at which the tip is stabilized. The edge enhancement is larger in the curves taken for a lower sample bias range, which corresponds to the tip being closer to the surface.

c. Resonant tunneling via image states. At metal surfaces, resonant tunneling into image states just below the vacuum level has been observed.[3] Such states are possible in insulators, too, except that their binding energy is reduced for a finite dielectric constant ϵ. Although tunneling into a bound image state is conceivable for the resonance in CaF_2, it cannot explain the resonance in CaF_1. That lies too far below the vacuum level.[9]

d. Enhancement of the density of states near the CBM. An interesting metal-semiconductor interaction has been predicted[26] that enhances the density of states near the band edges. Metal and insulator states form bonding-antibonding pairs that repel each other. Metal states near the bottom of the insulator band are pushed down and accumulate just below the band edge. In our case, such an enhancement of states might take place in the tip or at the underlying silicon.

In the following, we focus on option *a* and provide the simplest possible model for it. The agreement with the data is rather suggestive (compare Figs. 2 and 6), although it will be difficult to rule out the other options without getting into detailed calculations. The key idea is tunneling across two barriers in series, first across the vacuum gap and then through the insulator film. The standard theory of planar

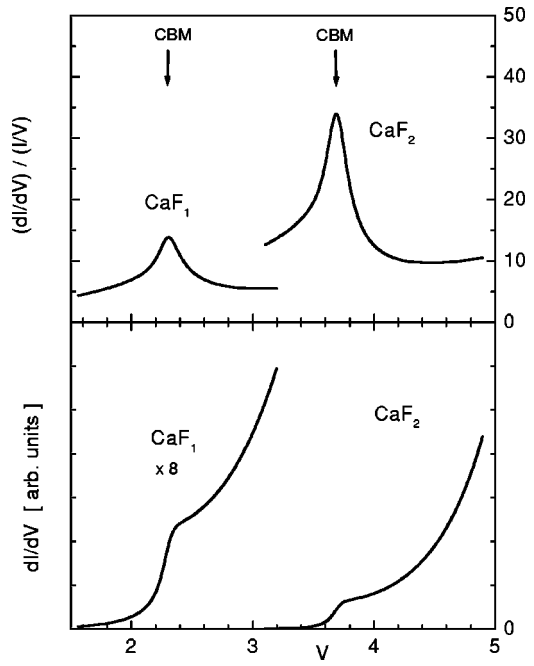

FIG. 6. Tunneling spectra obtained from a minimal model for tunneling through an insulator film [Eqs. (1)–(3)]. Calculated spectra are shown for CaF_2 and CaF_1, analogous to the data in Fig. 1.

tunneling[5,22–24] expresses the $I(V)$ curve in terms of the density of occupied states of the tip $D_{\mathrm{Tip}}(E)$, the transmission probability $T(E,V_S)$ from tip to sample, and the density of unoccupied states of the sample at an energy shifted by the bias voltage $D_{\mathrm{Sample}}(E+eV_S)$:

$$I(V_S)\sim\int D_{\mathrm{Sample}}(E+eV_S)T(E,V_S)D_{\mathrm{Tip}}(E)dE. \quad (1)$$

Here, the energy E is referenced to the Fermi level of the tip. We take the Si substrate as sample and the combination of the CaF_2 film and the vacuum gap as barrier. The simplest approximation for D_{Sample} and D_{Tip} is a constant,[27] multiplied by the Fermi function $f(E)$:

$$D_{\mathrm{Sample}}(E)\sim 1-f(E),$$
$$D_{\mathrm{Tip}}(E)\sim f(E), \quad (2)$$
$$f(E)=1/[\exp(E/kT)+1],$$

$kT=0.026\,\mathrm{eV}$ at room temperature. That reduces the problem to a calculation of transmission probability $T(E,V)$, which is decomposed into the component $T_{\mathrm{Vac}}(E,V_S)$ for the vacuum barrier and $T_{\mathrm{Ins}}(E,V_s)$ for the insulator film:

$$T(E,V_S)=T_{\mathrm{Vac}}(E,V_S)T_{\mathrm{Ins}}(E,V_S),$$
$$T_{\mathrm{Vac}}(E,V_S)=\exp[-2\sqrt{2m}/\hbar(\Phi-1/2eV_S-E)^{1/2}d_{\mathrm{Tip}}], \quad (3)$$
$$T_{\mathrm{Ins}}(E,V_S)=\begin{cases}\exp[-2\sqrt{2m}/\hbar(E_{\mathrm{CBM}}-eV_S-E)^{1/2}d_{\mathrm{Ins}}], & \text{for } eV_S+E<E_{\mathrm{CBM}},\\ 1, & \text{for } eV_S+E>E_{\mathrm{CBM}}.\end{cases}$$

E is the energy of a tunneling electron relative to the Fermi level of the tip, ranging from a few kT positive to $-eV_S$. V_S is the sample voltage, which is positive for tunneling into the conduction band. Φ represents the average work function between tip and insulator. For T_{Vac} we use the average barrier[5] $(\Phi-\frac{1}{2}eV_S)$ across the vacuum gap. E_{CBM} is the energy of the conduction-band minimum of the insulator relative to its Fermi level. Any voltage drop across the insulator is neglected. d_{Tip} is the distance of the tunneling tip from the insulator surface, and d_{Ins} the thickness of the insulator film. Most of these parameters can be estimated from independent measurements.[28] Only the position of the conduction band minimum E_{CBM} is adjusted to match the observed peak position in the $(dI/dV)/(I/V)$ spectra, which gives $E_{\mathrm{CBM}}-E_F=2.3\,\mathrm{eV}$ for CaF_1 and in $E_{\mathrm{CBM}}-E_F=3.7\,\mathrm{eV}$ for CaF_2.

Figure 6 shows the results of the model applied to our experimental conditions. It is to be compared with the data in Fig. 2. The general peak shape, and even the absolute peak height in the $(dI/dV)/(I/V)$ spectra is reproduced surprisingly well, given the simplicity of the model and the lack of adjustable parameters (apart from E_{CBM}). That suggests that we have captured the salient features of the resonance effect. Since the density of states is assumed to be constant, the resonance must be due to the change in the transmission near the conduction-band minimum. The model also provides predictions. For example, the height of the resonance scales with E_{CBM} and d_{Ins} approximately like

$$(dI/dV)/(I/V)_{\max}\approx 2.4\,(\mathrm{eV\,\AA})^{-1}d_{\mathrm{Ins}}E_{\mathrm{CBM}}. \qquad (4)$$

The resonance becomes stronger for larger E_{CBM}, making the technique particularly useful for insulators and wide-gap semiconductors. The calculated spectra are insensitive to the tip distance d_{Tip}, but they depend on the film thickness d_{Ins}. As the film becomes thicker, $(dI/dV)/(I/V)$ keeps increasing for energies inside the gap and diverges in the limit of an infinitely thick film. That is exactly the divergence problem that has plagued the interpretation of $(dI/dV)/(I/V)$ spectra from bulk semiconductors and has led to various schemes for artificially removing the divergence, such as adding a small constant to (I/V) or applying some amount of broadening to the (I/V) values.[24] The use of thin films in our work turns this difficulty around and converts it into an accurate tool for determining conduction-band minima and Schottky barriers in nanostructures. The value of $E_{\mathrm{CBM}}-E_F$, which corresponds to the *n*-type Schottky barrier, corresponds directly to the peak position in the $(dI/dV)/(I/V)$ spectrum.

Currently we are exploring refinements[29] of the minimal model given in Eqs. (1)–(3). They include a more realistic distribution of the voltage drop across insulator and vacuum. The two limiting cases are depicted in Fig. 4. The CaF_2 layer is conducting above the CBM, and the voltage drops completely across the vacuum gap (left). Tunneling deep inside the gap one approaches the electrostatic limit (right). In this case there is a significant voltage drop across the CaF_2 film, which is analogous to the tip-induced band bending discussed for semiconductors.[30,31] Another refinement is an explicit integration of the one-dimensional Schrödinger equation across the combined barrier, which yields more accurate transmission coefficients. That allows the inclusion of the image potential and the effects discussed in option *b*. The increasing influence of the image potential qualitatively explains why the peaks in the tunneling spectra slightly shift towards lower voltages when the tip approaches the surface. Further possible refinements are an effective mass for the conduction band of CaF_2 and the inclusion of three-dimensional effects, such as a finite escape cone.[22–24]

V. SUMMARY AND OUTLOOK

In summary, we have developed a chemical imaging method for insulators that has sub-nanometer resolution. Terrace height differences are eliminated completely from the chemical image. Different oxidation states can be distinguished (CaF_2 versus CaF_1). The method is based on a steep drop of the conductivity inside the gap, together with a newly found resonance in $(dI/dV)/(I/V)$ at the conduction-band minimum. A minimal model is given, which explains the resonance as an effect of tunneling across two barriers, the vacuum gap and the insulator film.

The method developed here should be useful for chemical imaging of insulators and wide-gap semiconductors. The conduction band edge of an individual nanostructure can be determined accurately from the resonance in the normalized conductance. Consequently, the local tunneling barrier and the band offset can be measured, which represent key parameters of potential devices, such as quantum dots using Coulomb blockade and single electron tunneling.

ACKNOWLEDGMENT

This work was supported by NSF under Grant Nos. DMR-9624753 and DMR-9632527.

*Permanent address: Institut für Festkörperphysik, Universität Hannover, D-30167 Hannover, Germany.

†Permanent address: Department of Physics, National Chung Cheng University, Taiwan, R.O.C.

[1] For a review see: T. Jung, F. J. Himpsel, R. R. Schlittler, and J. K. Gimzewski, *Chemical Information from Scanning Probe Microscopy and Spectroscopy*, Scanning Probe Microscopy, Analytical Methods, edited by R. Wiesendanger (Springer, Berlin 1998), Chap. 2, p. 11; For a possibility of chemical imaging of insulators by dynamic force microscopy see M. Bammerlin, R. Lüthi, E. Meyer, A. Baratoff, J. Lü, M. Guggisberg, Ch. Gerber, L. Howald, and H.-J. Güntherodt, Probe Microscopy **1**, 3 (1997).

[2] N. D. Browning, M. F. Chisholm, and S. J. Pennycook, Nature (London) **366**, 143 (1993); D. A. Muller, Y. Tzou, R. Raj, and J. Silcox, *ibid.* **366**, 725 (1993); P. E. Batson, *ibid.* **366**, 727 (1993).

[3] T. Jung, Y. W. Mo, and F. J. Himpsel, Phys. Rev. Lett. **74**, 1641 (1995); F. J. Himpsel, T. Jung, and P. F. Seidler, IBM J. Res. Dev. **42**, 33 (1998).

[4] R. Wiesendanger, M. Bode, R. Pascal, W. Allers, and U. D. Schwarz, J. Vac. Sci. Technol. A **14**, 1161 (1996).

[5] R. J. Hamers, *STM on Semiconductors*, Springer Series in Surface

Sciences Vol. 20 (Springer, Berlin, 1994), Chap. 5, p. 83; R. M. Feenstra, Surf. Sci. **299/300**, 965 (1994); J. A. Kubby and J. J. Boland, Surf. Sci. Rep. **26**, 61 (1996).

[6] H. W. M. Salemink, O. Albrektsen, and P. Koenraad, Phys. Rev. B **45**, 6946 (1992); S. Gwo, K.-J. Chao, C. K. Shih, K. Sadra, and B. G. Streetman, Phys. Rev. Lett. **71**, 1883 (1993).

[7] R. S. Goldman, R. M. Feenstra, C. Silfvenius, B. Stalnacke, and G. Landgren, J. Vac. Sci. Technol. B **15**, 1027 (1997).

[8] A. P. Alivisatos, Science **271**, 933 (1996); C. B. Murray, D. J. Norris, and M. G. Bawendi, J. Am. Chem. Soc. **115**, 8706 (1993).

[9] D. Rieger, F. J. Himpsel, U. O. Karlsson, F. R. Mc Feely, J. F. Morar, and J. A. Yarmoff, Phys. Rev. B **34**, 7295 (1986).

[10] Marjorie A. Olmstead, R. I. G. Uhrberg, R. D. Bringans, and R. Z. Bachrach, Phys. Rev. B **35**, 7526 (1987); Marjorie A. Olmstead, *Calcium Fluoride Growth on Silicon: From Chemisorption to Epitaxy*, Heteroepitaxial Systems, edited By Amy W. K. Liu and Michael Santos (World Scientific, Singapore 1998), Chap. 5.

[11] T. F. Heinz, F. J. Himpsel, E. Palange, and E. Burstein, Phys. Rev. Lett. **63**, 644 (1989); A. B. McLean and F. J. Himpsel, Phys. Rev. B **39**, 1457 (1989).

[12] S. Bouzidi, F. Coletti, J. M. Debever, J. L. Longueville, and P. A. Thiry, Appl. Surf. Sci. **56-58**, 821 (1992).

[13] R. M. Tromp and M. C. Reuter, Phys. Rev. Lett. **61**, 1756 (1988); J. Zegenhagen and J. R. Patel, Phys. Rev. B **41**, 5315 (1990). The former finds a ditance of 2.15 Å between the Ca and the top Si layer, latter being a distance of 2.34 Å. We use an average of 2.25 Å.

[14] J. Viernow, J.-L. Lin, D. Y. Petrovykh, F. M. Leibsle, F. K. Men, and F. J. Himpsel, Appl. Phys. Lett. **72**, 948 (1998); J.-L. Lin, D. Y. Petrovykh, J. Viernow, F. K. Men, D. J. Seo, and F. J. Himpsel, J. Appl. Phys. **84**, 255 (1998); J. Viernow, D. Y. Petrovykh, F. K. Men, A. Kirakosian, J.-L. Lin, and F. J. Himspel, Appl. Phys. Lett. (to be published); D. Y. Petrovykh, J. Viernow, J.-L. Lin, F. M. Leibsle, F. K. Men, A. Kirakosian, and F. J. Himpsel, J. Vac. Sci. Technol. (to be published).

[15] Ph. Avouris and R. Wolkow, Appl. Phys. Lett. **55**, 1074 (1989); The scanning tunneling spectrum in this work exhibits an onset at 1 V and a small peak at 2.2 V. The latter agrees with our CaF_1 peak, the former might be due to defects that show up as depressions in the topography. Our spectra are taken from atomically flat areas that do not exhibit such defects.

[16] R. Ludeke, A. Bauer, and E. Cartier, Appl. Phys. Lett. **66**, 730 (1995).

[17] V. P. LaBella, L. J. Schowalter, and C. A. Ventrice, J. Vac. Sci. Technol. B **15**, 1191 (1997); A peak in the ballistic electron emission microscopy spectrum of $Pt/CaF_2/Si(111)$ at 4.5 V is assigned to the density of states of the CaF_2 intralayer, which is consistent with our finding.

[18] M. T. Cuberes, A. Bauer, H. J. Wen, M. Prietsch, and G. Kaindl, J. Vac. Sci. Technol. B **12**, 2646 (1994).

[19] T. Nakayama, M. Katayama, G. Selva, and M. Aono, Phys. Rev. Lett. **72**, 1718 (1994).

[20] Touru Sumiya, Tadao Miura, and Shun-ichiro Tanaka, Surf. Sci. **357-358**, 896 (1996).

[21] The value of CBM-E_F of CaF_2 can be obtained from the reported (Refs. 9 and 10) band offsets of 2.5–4 eV between the CBM of CaF_2 and Si and a Fermi-level position of 0.5–1 eV below the CBM of Si. For CaF_1 values of CBM at $\overline{\Gamma}$ of 1.8 and 1.4 eV above E_F have been given in Refs. 11 and 12, respectively.

[22] C. B. Duke, *Tunneling in Solids*, Solid State Physics, Suppl. 10, edited by F. Seitz, D. Turnbull, and H. Ehrenreich (Academic, New York, 1969).

[23] N. D. Lang, Phys. Rev. B **34**, 5947 (1986).

[24] R. M. Feenstra, Phys. Rev. B **50**, 4561 (1994).

[25] The energy of the peak in the $(dI/dV)/(I/V)$ spectrum of CaF_1 would be consistent with the CBM of Si in the [111] direction, which corresponds to the L_1 point at 2.4 eV [see F. J. Himpsel, Surf. Sci. Rep. **12**, 1 (1990)]. Possibly, the L_1 state of Si hybridizes with the Ca 4*s* state.

[26] A. W. Overhauser, Appl. Phys. Lett. **54**, 2490 (1989).

[27] The assumption of a constant tip density of states is often made, lacking detailed knowledge of the tip states. The Si density of states has little structure at the energies under consideration, i.e., about 4 eV above the valence-band maximum.

[28] The parameters used in the calculation are estimated from independent measurements: For the work functions Φ of the tip and of CaF_2 we take 4 eV (compare Refs. 5 and 9). As tip distances we use typical values (Refs. 5 and 24) at the respective tip stabilization voltages, i.e., $d_{\mathrm{Tip}}=11$ Å at 4.3 V for CaF_2 and $d_{\mathrm{Tip}}=10$ Å at 3.5 V for CaF_1. The $(dI/dV)/(I/V)$ spectra are insensitive to variations in tip distance and work function, the (dI/dV) spectra change by a scaling factor. As sample thickness we use $d_{\mathrm{Ins}}=3.93$ Å for CaF_2 and $d_{\mathrm{Ins}}=2.7$ Å for CaF_1. The CaF_2 thickness is composed of 3.15 Å for the CaF_2 triple layer plus 0.78 Å for the F^- layer of the underlying CaF_1. The F^- is likely to exhibit the full CaF_2 gap because of its closed shell character. Using $d_{\mathrm{Ins}}=3.15$ Å instead for CaF_2 gives a resonance curve of similar shape but with the peak height reduced from 34 to 28. For the CaF_1 thickness we add half of the Si-Ca distance (Ref. 13) of 2.25 Å plus half of the CaF_2 thickness of 3.15 Å. These estimates are based on interfaces located halfway between lattice planes.

[29] D. Y. Petrovykh (unpublished).

[30] R. M. Feenstra and J. A. Stroscio, J. Vac. Sci. Technol. B **5**, 923 (1987).

[31] M. Weimer, J. Kramar, and J. D. Baldeschwieler, Phys. Rev. B **39**, 5572 (1989).